

This is the final unedited version of a manuscript accepted for publication.

The final edited version has been published in the Journal of Investigative Dermatology:

Szilveszter et al., J Invest Dermatol 2022 Apr, Vol. 142, No 4, Pages 1114-1125.

<https://doi.org/10.1016/j.jid.2021.09.019>

## Phospholipase Cy2 is essential for experimental models of epidermolysis bullosa acquisita

Kata P. Szilveszter<sup>1</sup>, Simon Vikár<sup>1</sup>, Ádám I. Horváth<sup>2,3</sup>, Zsuzsanna Helyes<sup>2,3,4</sup>, Miklós Sárdy<sup>5</sup> and Attila Mócsai<sup>1</sup>

<sup>1</sup>Department of Physiology, Semmelweis University School of Medicine, 1094 Budapest, Hungary; <sup>2</sup>Department of Pharmacology and Pharmacotherapy, University of Pécs, Medical School, 7624 Pécs, Hungary; <sup>3</sup>Molecular Pharmacology Research Group & Centre for Neuroscience, János Szentágothai Research Centre, University of Pécs, 7624 Pécs, Hungary; <sup>4</sup>PharmInVivo Ltd., 7629 Pécs, Hungary; <sup>5</sup>Department of Dermatology, Venereology and Dermatocology, Semmelweis University School of Medicine, 1085 Budapest, Hungary

Corresponding author:

Attila Mócsai, MD, PhD  
Department of Physiology  
Semmelweis University School of Medicine  
Tűzoltó utca 37-47, 1094 Budapest, Hungary  
Tel: +36-1-459-1500 Ext. 60-409  
Fax: +36-1-266-7480  
E-mail: [mocsai.attila@med.semmelweis-univ.hu](mailto:mocsai.attila@med.semmelweis-univ.hu)

Running title: PLCy2 in epidermolysis bullosa acquisita models

This work is licensed under a Creative Commons Attribution-NonCommercial-NoDerivatives 4.0 International License.

## ABSTRACT

Phospholipase C $\gamma$ 2 (PLC $\gamma$ 2) mediates tyrosine kinase-coupled receptor signaling in various hematopoietic lineages. Although PLC $\gamma$ 2 has been implicated in certain human and mouse inflammatory disorders, its contribution to autoimmune and inflammatory skin diseases is poorly understood. Here we tested the role of PLC $\gamma$ 2 in a mouse model of epidermolysis bullosa acquisita triggered by antibodies against type VII collagen (C7), a component of the dermo-epidermal junction. PLC $\gamma$ 2-deficient (*Plcg2*<sup>-/-</sup>) mice and bone marrow chimeras with a *Plcg2*<sup>-/-</sup> hematopoietic system were completely protected from signs of anti-C7-induced skin disease including skin erosions, dermal-epidermal separation and inflammation, despite normal circulating levels and skin deposition of anti-C7 antibodies. PLC $\gamma$ 2 was required for the tissue infiltration of neutrophils, eosinophils and monocytes/macrophages, as well as for the accumulation of proinflammatory mediators (including IL-1 $\beta$ , MIP-2 and LTB<sub>4</sub>) and reactive oxygen species. Mechanistic experiments revealed a role for PLC $\gamma$ 2 in the release of proinflammatory mediators and reactive oxygen species but not in the intrinsic migratory capacity of leukocytes. The PLC inhibitor U73122 inhibited dermal-epidermal separation of human skin sections incubated with human neutrophils in the presence of anti-C7 antibodies. Taken together, our results suggest a critical role for PLC $\gamma$ 2 in the pathogenesis of the inflammatory form of epidermolysis bullosa acquisita.

## INTRODUCTION

Epidermolysis bullosa acquisita is an autoimmune subepidermal blistering skin disease caused by autoantibodies targeting the dermal anchoring fibril type VII collagen (C7), a component of the dermal-epidermal junction (Schmidt and Zillikens, 2013; Baum et al., 2014; Turcan and Jonkman, 2015; Kridin et al., 2019; Egami et al., 2020). In case of the inflammatory form of epidermolysis bullosa acquisita, autoantibody deposition leads to local inflammation and disruption of the dermal-epidermal junction, mediated by complement activation and leukocyte (mainly eosinophil and neutrophil) infiltration. However, further details of its pathomechanism are poorly understood, limiting our options for therapeutic intervention (Kasperkiewicz and Schmidt, 2009; Maglie and Hertl, 2019).

Phospholipase C $\gamma$ 2 (PLC $\gamma$ 2) is primarily expressed in cells of hematopoietic origin and couples various tyrosine kinase-mediated signal transduction pathways to downstream signaling events (Faccio and Cremasco, 2010; Jackson et al., 2021). PLC $\gamma$ 2 plays important roles in B-cells, neutrophils, macrophages, mast cells, NK-cells, platelets and osteoclasts, and mediates signaling by B-cell-receptors, Fc-receptors, various integrins, C-type lectins and the collagen-receptor GpVI (Hashimoto et al., 2000; Wang et al., 2000; Wen et al., 2002; Wonerow et al., 2003; Nonne et al., 2005; Tassi et al., 2005; Caraux et al., 2006; Mao et al., 2006; Graham et al., 2007; Chen et al., 2008; Jakus et al., 2009; Kertész et al., 2012; Futosi et al., 2021).

Several lines of evidence suggest a role for PLC $\gamma$ 2 in autoimmune and inflammatory diseases. Gain-of-function mutations of PLC $\gamma$ 2 cause two human diseases, PLC $\gamma$ 2-associated antibody deficiency and immune dysregulation (PLAID) (Ombrello et al., 2012) and autoinflammation and PLAID (APLAID) (Zhou et al., 2012) characterized by immune dysregulation along with high prevalence of autoimmune and autoinflammatory diseases. Gain-of-function mutations of PLC $\gamma$ 2 also trigger complex inflammatory diseases in experimental mice (Yu et al., 2005; Abe et al., 2011), whereas PLC $\gamma$ 2-deficient (*Plcg2*<sup>-/-</sup>) mice are protected from disease development in various arthritis models (Cremasco et al., 2008; Jakus et al., 2009; Cremasco et al., 2010). Though skin pathology emerged in some of those studies (Yu et al., 2005; Abe et al., 2011; Zhou et al., 2012), the role of PLC $\gamma$ 2 in autoimmune and inflammatory skin diseases is poorly understood.

Tyrosine kinases are involved in diverse autoimmune and inflammatory skin diseases (Szilveszter et al., 2019). We have previously shown that myeloid Src-family kinases and the Syk tyrosine kinase are required for skin inflammation in a mouse model of epidermolysis bullosa acquisita (Kovács et al., 2014; Németh et al., 2017). Since PLC $\gamma$ 2 may lie downstream of Src-family kinases and Syk (Jakus et al., 2009; Németh et al., 2016), those studies suggest a potential role for PLC $\gamma$ 2 in development of autoimmune blistering skin diseases.

The above findings prompted us to test the role of PLC $\gamma$ 2 in an autoantibody-induced mouse model of the inflammatory form of epidermolysis bullosa acquisita. Our experiments revealed that PLC $\gamma$ 2 is indispensable for all tested aspects of disease development in this model, supposedly because of a role for PLC $\gamma$ 2 in the release of leukocyte proinflammatory mediators. A PLC inhibitor also blocked dermal-epidermal separation in a human ex vivo model, suggesting relevance to human epidermolysis bullosa acquisita.

## RESULTS

### PLC $\gamma$ 2 deficiency protects mice from autoantibody-induced skin blistering

To test the role of PLC $\gamma$ 2 in autoantibody-induced skin blistering, we injected wild-type and PLC $\gamma$ 2-deficient (*Plcg2*<sup>-/-</sup>) mice with polyclonal rabbit IgG antibodies against mouse type VII collagen (C7). As shown in Fig 1A, repeated systemic injection triggered severe skin erosion, crust formation and cutaneous inflammation in wild-type mice which was most prominent in the ears but was also seen around the nose and at various areas of the trunk. Importantly, no such changes could be observed on similarly treated *Plcg2*<sup>-/-</sup> mice. The time course of the percentage of the total affected skin area (Fig 1B), an overall clinical score taking into account the size and severity of each lesions (Fig 1C), as well as the percentage of the skin area showing erosions as a sign of blister eruption without the masking effect of other more severe secondary elementary lesions (Fig 1D) showed robust increase upon anti-C7 antibody treatment in wild-type but not in *Plcg2*<sup>-/-</sup> animals (Figs 1B-D;  $p=0.0011$ ,  $1.2\times 10^{-8}$ ,  $0.042$ , respectively). *Plcg2*<sup>-/-</sup> mice were also protected from anti-C7-induced increase of ear thickness as a more objective measure of disease severity (Fig 1E;  $p = 5.2\times 10^{-5}$ ).

Therefore, *Plcg2*<sup>-/-</sup> mice are protected from clinical signs of anti-C7-induced skin disease.

### Defective autoantibody-induced skin blistering in *Plcg2*<sup>-/-</sup> bone marrow chimeras

Breeding of *Plcg2*<sup>-/-</sup> mice is hindered by their male infertility (Ichise et al., 2016) and the lower-than-expected ratio of *Plcg2*<sup>-/-</sup> offspring from heterozygous mating (data not shown). To overcome those difficulties, we generated bone marrow chimeras with a *Plcg2*<sup>-/-</sup> hematopoietic system. Wild-type and *Plcg2*<sup>-/-</sup> bone marrow cells were transplanted into lethally irradiated wild-type recipients carrying the CD45.1 allele. Flow cytometric analysis of the donor-derived CD45.2 marker 4 weeks after transplantation revealed that practically all circulating neutrophils, eosinophils and monocytes were of donor origin (Fig 2A).

Repeated injection of anti-C7 antibodies triggered severe skin erosion, crust formation and cutaneous inflammation in wild-type bone marrow chimeras (Figs 2B-F). Importantly, similar to intact *Plcg2*<sup>-/-</sup> mice (Figs 1A-E), *Plcg2*<sup>-/-</sup> bone marrow chimeras were also completely protected from the clinical appearance of disease development (Fig 2B), as well as from all

quantitative measures of skin disease including skin erosions in our model (Figs 2C-F;  $p=6.9\times 10^{-14}$ ,  $9.3\times 10^{-11}$ , 0.0061 and 0.0063, respectively). Since such chimeras could be generated in significantly larger cohorts than intact *Plcg2*<sup>-/-</sup> mice, the following experiments were performed on such *Plcg2*<sup>-/-</sup> bone marrow chimeras.

Histological analysis of wild-type and *Plcg2*<sup>-/-</sup> bone marrow chimeras on Day 8 revealed anti-C7-induced dermal-epidermal separation and thickening of the ear tissue (likely due to both thickening of the epidermal layer and the infiltration of leukocytes) in wild-type but not in *Plcg2*<sup>-/-</sup> chimeras (Fig 2G). Further quantification revealed dramatic increase in dermal-epidermal separation upon anti-C7 treatment in wild-type chimeras, which was absent in *Plcg2*<sup>-/-</sup> mutants (Fig 2H;  $p=0.012$ ).

Therefore, *Plcg2*<sup>-/-</sup> bone marrow chimeras are protected from anti-C7-induced skin disease including histological separation at the dermo-epidermal interface.

### **Antibody levels and deposition**

We next tested whether the *Plcg2*<sup>-/-</sup> mutation reduces circulating levels or skin deposition of anti-C7 antibodies. As shown in Fig 3A, PLC $\gamma$ 2-deficiency even moderately increased circulating anti-C7 levels ( $p=9.0\times 10^{-6}$ ), possibly reflecting reduced consumption of circulating anti-C7 antibodies in the skin. Anti-C7 deposition along the dermo-epidermal junction was comparable between wild-type and *Plcg2*<sup>-/-</sup> mutants (Fig 3B). Therefore, the protection of *Plcg2*<sup>-/-</sup> mice in our model is likely not due to reduced circulating levels or tissue deposition of anti-C7 antibodies.

### **Leukocyte accumulation and migration**

Immunofluorescence staining on ear tissue sections from Day 8 showed abundant Ly6G-positive cells (supposedly neutrophils) in anti-C7-treated wild-type but not *Plcg2*<sup>-/-</sup> samples (Fig 4A). Flow cytometric analysis of digested ear tissue samples revealed robust accumulation of leukocytes (Fig 4B) including neutrophils (Fig 4C), eosinophils (Fig 4D) and monocytes/macrophages (Fig 4E) in anti-C7-treated wild-type chimeras. Importantly, no such infiltration could be observed in *Plcg2*<sup>-/-</sup> chimeras (Figs 4B-E;  $p=7.7\times 10^{-6}$ ,  $9.1\times 10^{-4}$ , 0.0097 and 0.0013, respectively). Therefore, PLC $\gamma$ 2 deficiency protects mice from leukocyte infiltration in our model.

To test whether the observed infiltration defect in *Plcg2*<sup>-/-</sup> animals is due to an impaired intrinsic migratory capacity of leukocytes, we generated mixed bone marrow chimeras with CD45.1-expressing WT and CD45.2-expressing WT or *Plcg2*<sup>-/-</sup> hematopoietic cells (giving rise to WT:WT and WT:*Plcg2*<sup>-/-</sup> mixed bone marrow chimeras, respectively), and subjected them to our skin disease model. All mice developed signs of skin disease, likely caused by the presence of wild-type cells (data not shown). On Day 8, we determined the ratio of CD45.1-

and CD45.2-expressing cells in the blood and in the digested ear samples, allowing us to compare the percentage of CD45.2 positive cells in the blood and in the tissue within the same animal. Representative histograms of CD45.2 expression within a neutrophil gate are shown in Figs 4F-G. As expected, the percentage of CD45.2-expressing wild-type neutrophils in WT:WT chimeras was comparable in the blood and the ear tissue (Fig 4F), although a modest reduction in the ear tissue (likely due to some technical issue) could be observed. Surprisingly, and in sharp contrast to the complete defect of neutrophil infiltration in *Plcg2*<sup>-/-</sup> chimeras (i. e. when all hematopoietic cells were of *Plcg2*<sup>-/-</sup> genotype; see Figs 4A and 4C), the percentage of CD45.2-expressing *Plcg2*<sup>-/-</sup> neutrophils in WT:*Plcg2*<sup>-/-</sup> chimeras was also comparable between the blood and the ear tissue (Fig 4G; although a moderate reduction in the ear tissue could again be seen). With other words, *Plcg2*<sup>-/-</sup> neutrophils were recruited to the ear tissue from the circulation as efficiently as wild-type cells. This was also confirmed by calculation of the recruitment efficiency of wild-type and *Plcg2*<sup>-/-</sup> neutrophils to the ear tissue (Fig 4H), and similar findings were observed for eosinophils and monocytes/macrophages tested in the same mice, as well (Fig 4H). Therefore, PLCγ2 is likely not required for the intrinsic ability of neutrophils, eosinophils and monocytes/macrophages to accumulate at the skin lesion site in our model.

Additional *in vitro* Transwell assays also revealed normal migration of *Plcg2*<sup>-/-</sup> neutrophils towards MIP-2 or LTB<sub>4</sub> (Figs 4I-J; p = 0.87 and 0.33, respectively).

Taken together, the protection of *Plcg2*<sup>-/-</sup> mutant mice from skin lesions are likely not due to a cell-autonomous migration defect of *Plcg2*<sup>-/-</sup> neutrophils, eosinophils or monocytes/macrophages.

### **PLCγ2 is required for the generation of the inflammatory microenvironment**

Since defective leukocyte infiltration may also be secondary to the inappropriate development of the inflammatory microenvironment, we tested the presence of proinflammatory mediators in the ear tissue of WT and *Plcg2*<sup>-/-</sup> bone marrow chimeras. As shown in the cytokine array in Fig 5A (see array map in Fig 5B), anti-C7 treatment triggered robust accumulation of a number of chemokines and cytokines in the ear of wild-type but not *Plcg2*<sup>-/-</sup> chimeras. This was confirmed by densitometric quantification of selected chemokines/cytokines with the most robust (>5-fold) increase in wild-type samples (Fig 5C). In addition, anti-C7 treatment strongly increased the concentration of IL-1β, MIP-2 and the lipid chemoattractant LTB<sub>4</sub> measured by ELISA in the ears of wild-type but not *Plcg2*<sup>-/-</sup> chimeras (Figs 5D-F; p=0.0044, 0.0046 and 1.1×10<sup>-4</sup>, respectively).

Since reactive oxygen species are involved in autoantibody-induced skin blistering (Chiriac et al., 2007), we tested *in vivo* reactive oxygen species production using a chemiluminescence-based *in vivo* imaging of myeloperoxidase activity. As shown in Figs 5G-

H, anti-C7 treatment triggered a robust chemiluminescence signal in wild-type but not *Plcg2*<sup>-/-</sup> chimeras ( $p = 3.3 \times 10^{-7}$ ).

Since neutrophils may contribute to the development of the inflammatory microenvironment (Mócsai, 2013; Németh and Mócsai, 2016) and likely mediate anti-C7-induced in vivo pathology (Chiriac et al., 2007; Csepregi et al., 2018), we have also tested the in vitro responsiveness of neutrophils to C7/anti-C7 immune complexes. As shown in Fig 5I, plating isolated neutrophils on C7/anti-C7 immune complex-coated surfaces triggered robust superoxide production from wild-type but not *Plcg2*<sup>-/-</sup> cells (Fig 5I;  $p = 3.5 \times 10^{-9}$ ). Similar results were seen when testing the spreading of the cells as a more general measure of cellular activation (Fig 5J). The *Plcg2*<sup>-/-</sup> mutation also blocked immune complex-induced release of MIP-2 and LTB<sub>4</sub> from neutrophils (Figs 5K-L;  $p = 0.027$  and  $1.3 \times 10^{-7}$ , respectively).

Taken together, PLC $\gamma$ 2 is required for the generation of various aspects of the inflammatory microenvironment upon anti-C7 treatment, which may explain the defective recruitment of leukocytes to the skin tissue. A role for PLC $\gamma$ 2 within neutrophils is likely at least partially responsible for those findings.

### Human in vitro studies

To extend the above findings to human pathology, we tested the effect of the phospholipase C (PLC) inhibitor U73122 on human neutrophils and in a human ex vivo skin separation assay.

Plating human neutrophils on C7/anti-C7 immune complex-coated surfaces triggered robust respiratory burst response which was inhibited by U73122 in a concentration-dependent manner, reaching complete inhibition at 10  $\mu$ M concentration (Fig 6A). U73122 also blocked spreading of human neutrophils on a C7/anti-C7 immune complex-coated surface (Fig 6B). Those results mirror the phenotype of *Plcg2*<sup>-/-</sup> mouse neutrophils (Figs 5I-J).

Finally, we set up a human ex vivo dermal-epidermal separation assay by preincubating frozen healthy human skin sections with the above anti-C7 antibodies, followed by further incubation with healthy human neutrophils and normal human plasma as a source of complement components. As shown in Fig 6C, anti-C7 treatment led to the accumulation of neutrophils at the dermo-epidermal junction and skin separation between the dermal and epidermal layers in vehicle-treated samples. Importantly, U73122 added during the incubation of the skin sections with neutrophils strongly inhibited dermal-epidermal separation in this assay (Fig 6C). This was confirmed by quantification of skin separation along the dermal-epidermal interface, showing robust anti-C7-induced dermal-epidermal separation in vehicle-treated but not U73122-treated samples (Fig 6D;  $p = 0.020$ ).

Taken together, the PLC inhibitor U73122 strongly inhibits C7/anti-C7 immune complex-induced activation of human neutrophils and anti-C7-induced ex vivo dermal-epidermal separation of human skin sections.

## DISCUSSION

We show that PLC $\gamma$ 2 is critical for the development of a widely used mouse model of the inflammatory form of epidermolysis bullosa acquisita. Our results improve our understanding of the pathomechanism and identify a possible therapeutic target of this rare autoimmune blistering skin disease.

The inflammatory form of epidermolysis bullosa acquisita and its anti-C7-induced mouse model are characterized by signs of dermal-epidermal separation (including blistering and skin erosions) along with inflammatory features such as leukocyte infiltration and accumulation of proinflammatory mediators. The fact that the *Plcg2*<sup>-/-</sup> mutation abrogated both dermal-epidermal separation (Figs 1A, 1D, 2B, 2E and 2G-H) and inflammation (Figs 4A-E and 5A-H) suggests that PLC $\gamma$ 2 plays an important role in a common step of disease development. Since PLC $\gamma$ 2 is an intracellular signaling molecule and complete protection from disease development could be observed in chimeric mice with a *Plcg2*<sup>-/-</sup> hematopoietic system (Fig 2), this common step is likely mediated by cells of hematopoietic origin (rather than cell-free processes such as the classical pathway of complement activation). Though our experiments do not allow us to identify the cell type(s) requiring PLC $\gamma$ 2 expression during disease development, preliminary lineage-specific deletion experiments point to a role for PLC $\gamma$ 2 within neutrophils (unpublished observations), which would also be in line with the critical role of neutrophils in this model (Chiriac et al., 2007; Csepregi et al., 2018). Nevertheless, we cannot exclude the role of PLC $\gamma$ 2 within eosinophils, monocytes/macrophages or other non-lymphoid cells, whereas our experimental design (passive transfer of anti-C7-antibodies) and the absence of PLC $\gamma$ 2 in circulating T-cells (unpublished observation) argue against a critical role for PLC $\gamma$ 2 in B- or T-cells.

We have performed a large number of experiments to reveal how PLC $\gamma$ 2 mediates anti-C7-induced disease development. It is unlikely that PLC $\gamma$ 2 plays a major role in myeloid cell development since the *Plcg2*<sup>-/-</sup> mutation did not reduce the circulating number or the critical cell surface marker expression (including various  $\beta$ <sub>2</sub>-integrin chains and Fc $\gamma$ -receptors) of major myeloid-lineage cells ((Jakus et al., 2009) and unpublished observations). PLC $\gamma$ 2 was not required for the maintenance of circulating anti-C7 antibody levels or antibody deposition at the dermal-epidermal interface (Fig 3). Though PLC $\gamma$ 2 deficiency abrogated the accumulation of all tested myeloid cell types in the skin of anti-C7-treated mice (Figs 4A-E), this was likely not due to a cell-intrinsic migration defect since *Plcg2*<sup>-/-</sup> neutrophils, eosinophils and monocytes/macrophages were recruited normally to the skin when wild-type cells were

also present (Figs 4F-H), and *Plcg2*<sup>-/-</sup> neutrophils showed normal migration in in vitro Transwell assays (Figs 4I-J). On the other hand, PLCγ2 deficiency abrogated various aspects of the generation of an inflammatory microenvironment such as tissue accumulation of proinflammatory mediators (Figs 5A-F) or in vivo reactive oxygen species production (Figs 5G-H). *Plcg2*<sup>-/-</sup> neutrophils also failed to respond to C7/anti-C7 immune complexes (Figs 5I-L). The most plausible explanation of all those findings is that anti-C7 antibody deposition at the dermal-epidermal junction activates neutrophils (and possibly other myeloid-lineage cells) which release proinflammatory mediators, thus recruiting further leukocytes and amplifying the inflammatory response. This would be in line with the feedback amplification of neutrophil function in other disease processes (Németh and Mócsai, 2016) and the biphasic nature of neutrophil recruitment upon anti-C7 administration (Hundt et al., 2020). PLCγ2 deficiency likely blocks the release of proinflammatory mediators and therefore abrogates the entire feedback amplification loop, including recruitment of additional leukocytes. It should be noted that LTB<sub>4</sub> has been proposed to be a critical driver of neutrophil recruitment in a model similar to ours (Sezin et al., 2017). The role of PLCγ2 in the tissue accumulation of LTB<sub>4</sub> (Fig 5F) and the *in vitro* release of LTB<sub>4</sub> from immune complex-stimulated neutrophils (Fig 5L) in our hands suggest that blocking an LTB<sub>4</sub>-mediated feedback amplification loop is at least partially responsible for the defective skin disease in *Plcg2*<sup>-/-</sup> mutants. Besides the role of PLCγ2 in this inflammatory amplification loop, it likely also plays a direct role in degradation of the dermal-epidermal junction, as suggested by the inhibitory effect of U73122 on ex vivo dermal-epidermal separation (Figs 6C-D).

Besides detailed genetic experiments in mice, we have also performed experiments on human cells and tissues using a pharmacological approach. The inhibitory effect of U73122 on the responses of human neutrophils to C7/anti-C7 immune complexes (Figs 6A-B) and on the *ex vivo* dermal-epidermal separation of human skin sections in the presence of human neutrophils and anti-C7 antibodies (Figs 6C-D) are in line with a critical role for PLCγ2 in the inflammatory form of epidermolysis bullosa acquisita.

It is interesting to note that rare PLCγ2 gain-of-function mutations also caused manifestations resembling human epidermolysis bullosa acquisita and its mouse model. Both originally described APLAID patients had epidermolysis bullosa-like eruptions, skin lesions infiltrated by neutrophils and eosinophils, as well as corneal blistering that progressed to corneal erosions and ulceration (Zhou et al., 2012). Bullous skin eruptions and corneal lesions were also prominent findings in other patients with APLAID-like diseases caused by other gain-of-function missense mutations of PLCγ2 (Neves et al., 2018; Moran-Villasenor et al., 2019; Martin-Nalda et al., 2020; Novice et al., 2020). In addition, both the *Ali5* and *Ali14* gain-of-function mutations of mouse PLCγ2 led to severe skin inflammation with granulocytic and

eosinophilic infiltrates (Yu et al., 2005; Abe et al., 2011). Those reports further support a role for PLC $\gamma$ 2 in the pathogenesis of the inflammatory form of epidermolysis bullosa acquisita.

A few limitations of our study should also be mentioned. Autoantibodies in the non-inflammatory form of epidermolysis bullosa acquisita likely directly block the molecular interactions of type VII collagen, weakening the dermo-epidermal junction without a significant inflammatory component. Given the very different molecular pathomechanism, results of our experiments should not be directly extrapolated to that other disease process. Also, we cannot exclude the role of PLC $\gamma$ 2 expressed within cell types of non-hematopoietic origin (e.g. fibroblasts or keratinocytes) in the pathogenesis of the inflammatory form of epidermolysis bullosa acquisita. However, the dominantly hematopoietic expression of PLC $\gamma$ 2 (Faccio and Cremasco, 2010; Jackson et al., 2021) and the mostly normal development of a mechanistically similar autoantibody-induced arthritis model in *Plcg2*<sup>-/-</sup> recipients transplanted with wild-type bone marrow cells (Futosi et al., 2021) make that possibility rather unlikely.

Taken together, our studies identify an important component of the development of the inflammatory form of epidermolysis bullosa acquisita and point to a potential molecular target of future pharmacological intervention.

## **MATERIALS AND METHODS**

### **Animals**

Mice carrying the *Plcg2*<sup>tm1Jni</sup> (referred to as *Plcg2*<sup>-</sup>) mutation inactivating the PLC $\gamma$ 2-encoding gene (Wang et al., 2000) were obtained from James Ihle (St. Jude Children's Research Hospital) and were maintained by heterozygous breeding to obtain *Plcg2*<sup>-/-</sup> animals. Genotyping was performed by allele-specific PCR from tail DNA. *Plcg2*<sup>+/+</sup> littermates or wild-type C57BL/6 mice from our colony were used as wild-type control animals. For bone marrow transplantation, recipients carrying the CD45.1 allele on the C57BL/6 genetic background (B6.SJL-*Ptprc*<sup>a</sup>; purchased from the Jackson Laboratory, Bar Harbor, ME) were lethally irradiated by 11 Gy from a <sup>137</sup>Cs source using a Gamma-Service Medical D1 irradiator, followed by intravenous injection of unfractionated donor bone marrow cells. Repopulation of the hematopoietic system was tested by flow cytometry 4 weeks after transplantation (Jakus et al., 2010). Mice were kept in individually sterile ventilated cages (Tecniplast, Buguggiate, Italy) under specific pathogen-free conditions and transferred to a conventional facility for experiments. All animal experiments were approved by the Animal Experimentation Review Board of Semmelweis University or of the University of Pécs.

### **Autoantibody-induced skin blistering**

The murine model of the inflammatory form of human epidermolysis bullosa acquisita was induced by systemic injection of antibodies against collagen type VII (Sitaru et al., 2005).

GST-tagged (GST-C7) and His-tagged (His-C7) fusion proteins containing a fragment of the immunodominant NC1 domain of mouse C7 were expressed in *E. coli* BL21 using plasmids obtained from Cassian Sitaru (University of Freiburg, Germany), and purified using glutathione- or Ni<sup>2+</sup>-based affinity chromatography, respectively (Sitaru et al., 2005; Csorba et al., 2010). C7 fragment was obtained by cleavage with PreScission protease (GE Healthcare, Chicago, IL). Polyclonal anti-C7 antibodies were produced by immunizing rabbits at the Hungarian National Agricultural Innovation Center with GST-C7, followed by total IgG preparation using protein G-based affinity chromatography (rProteinG agarose, Thermo Fischer Scientific, Waltham, MA). Reactivity of rabbit sera was tested by ELISA using His-C7 as the capturing antigen to exclude anti-GST signals (Csorba et al., 2010).

For the induction of skin blistering, 12 mg anti-C7 or PBS (as control) was injected subcutaneously under isoflurane anesthesia on Days 0, 2, 4, 6, and 8 (60 mg total IgG/mouse) (Sitaru et al., 2005; Németh et al., 2017). Disease onset and progression was followed by evaluation of the size of total affected skin area, the size of erosions alone, and a severity score reflecting both lesion size and severity (alopecia, scaling, induration, erosion and crust formation in increasing order) added together into a single score. Ear thickness was measured by a spring-loaded caliper (Kroeplin). Serum anti-C7 levels were determined on Days 0, 8 and 14 by ELISA using His-C7 as the capturing antigen.

### **Histological analyses in mice**

Control and anti-C7 treated chimeras were sacrificed on Day 8. Ear tissue was removed, fixed in 4% paraformaldehyde, dehydrated and embedded in paraffin. Sections were stained with hematoxylin-eosin or immunostained using antibodies against Ly6G (clone 1A8, BD Biosciences, San Jose, CA) followed by fluorescently labeled secondary antibodies.

For anti-C7 deposition assays, chimeras were injected once with 4 mg anti-C7 or normal rabbit IgG. 24 h later, the mice were sacrificed and ear cryosections were stained with Alexa Fluor 488-labeled anti-rabbit IgG or irrelevant anti-rat IgG as control.

### **Analysis of leukocyte infiltration and inflammatory mediators in the ear**

Control and anti-C7 treated chimeras were sacrificed on Day 8. Ear tissue was removed and digested with Liberase TM (Roche, Basel, Switzerland) to obtain single-cell suspensions for flow cytometry. Cell-free supernatants of the digested samples were used to evaluate inflammation-related chemokines and cytokines using a mouse cytokine antibody array kit (Panel A) or commercial IL-1 $\beta$ , MIP-2 or LTB<sub>4</sub> ELISA kits (all from R&D Systems, Minneapolis, MN) as described (Kovács et al., 2014).

## **Flow cytometry**

Blood samples or single-cell suspensions of digested ear tissues were washed, stained with antibodies against CD11b (M1/70), CD45.2 (104), Ly6G (1A8) and Siglec F (E50-2440) and then resuspended in FACS lysing solution (all reagents from BD Biosciences). Specified volumes were used throughout, allowing a precise determination of absolute cell counts. Flow cytometry was performed on a FACSCalibur flow cytometer (BD Biosciences) and analyzed by FCS Express 6 (De Novo Software). Neutrophils were identified as CD11b<sup>+</sup>Ly6G<sup>+</sup>Siglec-F<sup>-</sup>, eosinophils as CD11b<sup>+</sup>Ly6G<sup>-</sup>Siglec-F<sup>+</sup> and monocytes/macrophages as CD11b<sup>+</sup>Ly6G<sup>-</sup>Siglec-F<sup>-</sup> cells within their typical FSc/SSc gates.

## **Competitive *in vivo* migration**

*In vivo* migration of neutrophils, eosinophils and monocytes/macrophages was investigated in mixed bone marrow chimeras (Mócsai et al., 2002; Jakus et al., 2009; Kovács et al., 2014). Briefly, CD45.1-expressing wild-type recipients were transplanted with CD45.1-expressing wild-type and CD45.2-expressing wild-type or *Plcg2*<sup>-/-</sup> bone marrow at varying ratios. After bone marrow repopulation, skin blistering was induced by anti-C7 antibodies. On Day 8, single-cell suspensions were obtained from blood and from ear tissues and the percentage of CD45.2-expressing cells was assessed by flow cytometry. Relative migration was calculated as described (Jakus et al., 2009).

## ***In vivo* chemiluminescence assay**

*In vivo* MPO activity was detected using a chemiluminescence assay (Gross et al., 2009; Kovács et al., 2014). Control and anti-C7 treated chimeras were injected intraperitoneally with 150 mg/kg luminol sodium salt (Gold Biotechnology) on Day 8. Luminescence images were captured by IVIS Lumina II imaging system (PerkinElmer, Waltham, MA; 120 s acquisition, Binning=8, F/Stop=1) under 120/6 mg/kg i. p. ketamine-xylazine anesthesia. For quantitative analysis, total radiance values (total photon flux/s) were used from standardized regions of interest of the ears.

## **Isolation and *in vitro* activation of mouse neutrophils**

Mouse neutrophils were isolated from the bone marrow by Percoll (GE Healthcare) gradient centrifugation (Mócsai et al., 2003). Neutrophil assays were performed at 37 °C in Hank's balanced salt solution (HBSS; Lonza, Basel, Switzerland) supplemented with 20 mM HEPES, pH 7.4 or in DMEM (Sigma-Aldrich, St. Louis, MO; for the measurement of LTB<sub>4</sub> release).

*In vitro* migration was assessed by a Transwell assay system (Mócsai et al., 2002; Jakus et al., 2009). Transwell inserts with 5 µm pore size (Corning, Acton, MA) were precoated with

fibrinogen, filled with neutrophil suspension and placed into media containing 100 ng/ml MIP-2 (PeproTech GmbH, Hamburg, Germany) or 50 ng/ml LTB<sub>4</sub> (Santa Cruz Biotechnology, Dallas, TX). After 1 h incubation, ratio of transmigrated neutrophils into the lower compartment was determined by an acid phosphatase assay (Mócsai et al., 2002).

Immobilized immune complex-coated surfaces were obtained by binding C7 at 20 µg/ml to Nunc MaxiSorp F96 plates (Thermo Fisher Scientific), blocking, and then treating with anti-C7 at 300 µg/ml. C7 or anti-C7 treatment alone served as controls. Superoxide release was followed by a cytochrome c reduction test (Németh et al., 2010). Neutrophil spreading was examined using phase contrast microscopy (Leica DMI600 B fluorescence microscope, Wetzlar, Germany) after 30 min stimulation. For the analysis of mediator release, neutrophils were stimulated for 1 h (LTB<sub>4</sub>) or 4 h (MIP-2). Supernatants were collected and measured by commercial ELISA kits described above.

### **Isolation and *in vitro* activation of human neutrophils**

Human neutrophils were isolated from venous blood of healthy volunteers by Ficoll (GE Healthcare) gradient centrifugation (Futosi et al., 2012). All experiments on human samples were approved by the Scientific and Research Ethics Committee of the Medical Research Council of Hungary.

The PLC inhibitor U73122 (Selleck Chemicals, Houston, TX) was dissolved in dimethylformamide (DMF). Isolated neutrophils were pretreated at 37 °C for 20 min with vehicle (DMF) or U73122 at the indicated concentrations. The final vehicle- and inhibitor-treated samples contained 0.05% DMF. *In vitro* neutrophil assays were performed at 37 °C in HBSS. Superoxide release and cell spreading on immobilized C7/anti-C7 immune complex surfaces were measured as described above.

### ***Ex vivo* human skin separation assay**

Neutrophil-mediated dermal-epidermal separation in cryosections of healthy human skin was performed essentially as described (Gammon et al., 1982). Healthy human skin samples were obtained from surgical interventions. Cryosections were made, incubated with 6 mg/ml anti-C7 or normal rabbit IgG for 1.5 h and washed. Neutrophils isolated from healthy donors were diluted in RPMI (Biosera) to 10<sup>7</sup>/ml in the presence of human plasma, treated with vehicle (0,05% DMF) or 10 µM U73122, preincubated at 37 °C and then plated over the antibody-treated cryosections. After 1.5 h incubation at 37 °C, sections were washed, fixed and stained with H&E.

## **Presentation of the data and statistical analysis**

Experiments were performed the indicated number of times. Quantitative graphs and kinetic curves show mean and SEM from all individual mice or samples from the indicated number of experiments. Statistical analyses were carried out by the STATISTICA software using two-way (factorial) ANOVA, with treatment and genotype being the two independent variables. One-way ANOVA was used to evaluate in vivo migration experiments. Area under the curve was used for statistical analysis in kinetic measurements. p values below 0.05 were considered statistically significant.

## **DATA AVAILABILITY**

No datasets were generated or analyzed during the current study.

## **ACKNOWLEDGMENT**

We thank Edina Simon, Nikolett Szénási and Tamás Kiss for expert technical assistance; Péter Major and László Hiripi for help with rabbit immunization; Tamás Németh for intellectual advice; Lukács Lesinszki for help with initial experiments; Cassian Sitaru for C7 expression plasmids and helpful suggestions; and James Ihle for transgenic mice. This work was supported by the Hungarian National Scientific Research Fund (NKFIH-OTKA Grants No. KKP129954 and K119653 to A. M.), the Hungarian National Research, Development and Innovation Office (NVKP\_16-2016-1-0039, to A. M.), the European Union's H2020 IMI2 program (RTCure project; grant no. 777357 to A.M.), the Hungarian Ministry of National Economy (VEKOP-2.3.2-16-2016-00002 to A. M., EFOP-3.6.3-VEKOP-16-2017-00009 to K. P. S. and GINOP-2.3.2-15-2016-00048 to Z. H.) and the European Social Fund (EFOP-3.6.1-16-2016-00004). The imaging studies were performed at the Small Animal Imaging Core Facility of the Szentágotthai Research Centre of the University of Pécs.

## **ORCIDs**

Kata P. Szilveszter: <http://orcid.org/0000-0001-6185-7233>

Simon Vikár: <http://orcid.org/0000-0003-3681-0278>

Ádám I. Horváth: <http://orcid.org/0000-0002-4724-8201>

Zsuzsanna Helyes: <http://orcid.org/0000-0003-2435-4367>

Miklós Sárdy: <http://orcid.org/0000-0003-4306-5093>

Attila Mócsai: <http://orcid.org/0000-0002-0512-1157>

## **AUTHOR CONTRIBUTIONS**

Conceptualization: KPS, AM. Investigation: KPS, SV, ÁIH. Resources: MS, ZH. Writing: KPS, AM. Supervision: AM.

## **CONFLICT OF INTEREST DISCLOSURES**

The authors have no conflicting financial interests.

## **ETHICS STATEMENT**

All animal experiments were approved by the Animal Experimentation Review Board of Semmelweis University or of the University of Pécs. Human experiments were approved by the Scientific and Research Ethics Committee of the Medical Research Council of Hungary. Human subjects provided written, informed consent before blood sampling.

## FIGURE LEGENDS

### Figure 1

#### ***Plcg2*<sup>-/-</sup> mice are protected from autoantibody-induced skin blistering**

Wild-type (WT) and *Plcg2*<sup>-/-</sup> mice were injected by PBS (Control) or polyclonal anti-C7 antibodies every second day until Day 8. Disease development was followed by photographing on Days 12-15 (a), scoring the extent of total affected skin area (b), severity of lesions (c), percentage of erosions (d) and ear thickness measurements (e). Green arrows in panel (a) indicate erosions. Photographs are representative of, and quantitative data show mean and SEM from, 5-9 mice per group from 4-5 individual experiments except control-treated *Plcg2*<sup>-/-</sup> mice where data of 3 mice from 2 experiments are shown due to the limited availability of *Plcg2*<sup>-/-</sup> animals.

### Figure 2

#### **Autoantibody-induced skin blistering is abrogated in *Plcg2*<sup>-/-</sup> bone marrow chimeras**

(a) Flow cytometric analysis of the donor-specific CD45.2 marker 4 weeks after bone marrow transplantation in major circulating myeloid cell types. Histograms are representative of 12-23 chimeras per group from 2-3 independent experiments. (b-f) Skin blistering was induced in wild-type (WT) and *Plcg2*<sup>-/-</sup> chimeras by systemic injection of PBS (Control) or anti-C7 antibodies. Disease development was followed by photographing on Days 12-14 (b), scoring the extent of total affected skin area (c), severity of lesions (d), percentage of erosions (e) and ear thickness measurements (f). Green arrows in panel (b) indicate erosions. (g, h) Ear samples were obtained from wild-type (WT) and *Plcg2*<sup>-/-</sup> bone marrow chimeras on Day 8. Paraffin embedded sections were generated and stained with hematoxylin and eosin (g) followed by quantification of the extent of dermal-epidermal (D-E) separation (h). Black arrows in panel (g) indicate D-E separation. Scale bar: 100  $\mu$ m. Photographs (b, g) are representative of, and quantitative data (c-e, h) show mean and SEM from, 5-12 mice per group from 3-5 independent experiments. Data in panel (f) show mean and SEM of 3-4 chimeras per group from 2 independent experiments.

### Figure 3

#### **Serum anti-C7 antibody level and deposition along the dermal-epidermal junction**

(a) Serum level of injected anti-C7 antibodies of wild-type (WT) and *Plcg2*<sup>-/-</sup> chimeras were measured by indirect ELISA. Blood samples were obtained on Days 0, 8 and 14. Bar graphs show mean and SEM from 8 mice per group from 3 independent experiments. (b) Wild-type and *Plcg2*<sup>-/-</sup> chimeras were injected with 4 mg anti-C7. After 24h, immunofluorescent staining of deposited rabbit anti-C7 antibodies was obtained on cryosections of ears using Alexa Fluor

488-labeled anti-rabbit IgG or irrelevant antibody. Histological images are representative of 3 mice per group from 3 independent experiments (**b**). Scale bar: 60  $\mu$ m.

#### Figure 4

##### Defective leukocyte accumulation but normal cell-autonomous migration

(**a-e**) Wild-type (WT) and *Plcg2*<sup>-/-</sup> bone marrow chimeras were subjected to skin blistering and ear tissues were obtained on Day 8. Dermal infiltration of neutrophils was examined in paraffin embedded ear sections stained with anti-Ly6G followed by Alexa Fluor 488-labeled secondary antibodies or secondary antibodies alone (**a**). (**b-e**) Quantitative analysis of different leukocyte populations was performed in digested ear samples using flow cytometry. (**f, h**) Mixed bone marrow chimeras containing CD45.1-expressing WT and CD45.2-expressing WT (WT:WT) or *Plcg2*<sup>-/-</sup> (WT: *Plcg2*<sup>-/-</sup>) bone marrow were subjected to skin blistering. Quantitative analysis of myeloid cells in the blood and in digested ear samples was performed by flow cytometry. Ratio of CD45.1- and CD45.2-expressing cells in the 3 major myeloid subtypes was determined in the blood and the ear. Panels **f** and **g** show the expression of CD45.2 in neutrophils in a WT:WT and a WT: *Plcg2*<sup>-/-</sup> mixed bone marrow chimera, respectively. Panel **h** shows the relative migration of CD45.2-expressing cells compared to CD45.1-expressing wild-type cells within the same animal. (**i, j**) In vitro migration of neutrophils isolated from bone marrow of wild-type and *Plcg2*<sup>-/-</sup> chimeras was tested in a Transwell migration assay towards 100 ng/ml MIP-2 (**i**) or 50 ng/ml LTB<sub>4</sub> (**j**). Histological images (**a**) and histograms (**f, g**) are representative of 3-8 mice from 2 independent experiments. Scale bar: 30  $\mu$ m (**a**). Bar graphs (**b-e, h-j**) show mean and SEM from 3-10 mice per group from 2-4 independent experiments.

#### Figure 5

##### PLCY2 deficiency abrogated the generation of the inflammatory microenvironment

(**a-f**) Cell-free supernatants were obtained from the ear tissue of wild-type (WT) and *Plcg2*<sup>-/-</sup> bone marrow chimeras on Day 8. The presence of several chemokines and cytokines was tested using a semiquantitative cytokine array (**a-c**) and quantitative ELISA for IL-1 $\beta$  (**d**), MIP-2 (**e**) and LTB<sub>4</sub> (**f**). Representative images (**a**) and the layout of analytes (**b**) in the cytokine array are presented together with integrated densitometry values normalized to WT control samples (**c**) from 2 independent experiments. (**g**) In vivo myeloperoxidase activity was tested by chemiluminescence imaging after intraperitoneal injection of luminol on Day 8. Photon flux intensity was quantified in defined regions of the ears (**h**). Chemiluminescence images are representative of, and quantitative data show mean and SEM from 7-8 animals per group from 2 independent experiments. (**i-l**) In vitro activation of wild-type and *Plcg2*<sup>-/-</sup> bone marrow-derived neutrophils. Superoxide release (**i**), spreading (**j**), MIP-2 production (**k**) and LTB<sub>4</sub> release (**l**) of neutrophils were measured upon plating the cells onto C7/anti-C7 immune

complex-coated or antigen (C7)-coated control surfaces. Images in panel **j** are representative of, and quantitative data (**i, k, l**) show mean and SEM from, at least 3 independent experiments. Scale bar: 50  $\mu\text{m}$ .

## **Figure 6**

### **U73122 blocks immune complex-mediated activation of human neutrophils and ex vivo dermal-epidermal separation**

**(a, b)** Human neutrophils were activated by immobilized C7/anti-C7 immune complexes in vitro. Superoxide release (**a**) was measured in neutrophils treated by the indicated concentrations of the PLC inhibitor U73122. Cell spreading (**b**) was tested in neutrophils treated with either 0.05% DMF (vehicle) or 1  $\mu\text{M}$  U73122. **(c, d)** Ex vivo dermal-epidermal separation was evaluated in cryosections of normal IgG- or anti-C7-treated healthy human skin. Sections were incubated with 0.05% DMF (vehicle) or 10  $\mu\text{M}$  U73122-treated neutrophils for 1.5 h, followed by staining with H&E (**c**). The percentage of dermal-epidermal separation is shown in panel **d**. Microscopic images are representative of, and quantitative data show mean and SEM from, at least 3 independent experiments. Scale bar: 50  $\mu\text{m}$ .

## REFERENCES

- Abe K, Fuchs H, Boersma A, Hans W, Yu P, Kalaydjiev S, et al. A novel N-ethyl-N-nitrosourea-induced mutation in phospholipase Cy2 causes inflammatory arthritis, metabolic defects, and male infertility in vitro in a murine model. *Arthritis Rheum* 2011;63:1301-11.
- Baum S, Sakka N, Artsi O, Trau H, Barzilai A. Diagnosis and classification of autoimmune blistering diseases. *Autoimmun Rev* 2014;13:482-9.
- Caraux A, Kim N, Bell SE, Zompi S, Ranson T, Lesjean-Pottier S, et al. Phospholipase Cy2 is essential for NK cell cytotoxicity and innate immunity to malignant and virally infected cells. *Blood* 2006;107:994-1002.
- Chen Y, Wang X, Di L, Fu G, Bai L, Liu J, et al. Phospholipase Cy2 mediates RANKL-stimulated lymph node organogenesis and osteoclastogenesis. *J Biol Chem* 2008;283:29593-601.
- Chiriac MT, Roesler J, Sindrilaru A, Scharffetter-Kochanek K, Zillikens D, Sitaru C. NADPH oxidase is required for neutrophil-dependent autoantibody-induced tissue damage. *J Pathol* 2007;212:56-65.
- Creмасco V, Graham DB, Novack DV, Swat W, Faccio R. Vav/Phospholipase Cy2-mediated control of a neutrophil-dependent murine model of rheumatoid arthritis. *Arthritis Rheum* 2008;58:2712-22.
- Creмасco V, Benasciutti E, Cella M, Kisseleva M, Croke M, Faccio R. Phospholipase Cy2 is critical for development of a murine model of inflammatory arthritis by affecting actin dynamics in dendritic cells. *PLoS One* 2010;5:e8909.
- Csepregi JZ, Orosz A, Zajta E, Kása O, Németh T, Simon E, et al. Myeloid-specific deletion of Mcl-1 yields severely neutropenic mice that survive and breed in homozygous form. *J Immunol* 2018;201:3793-803.
- Csorba K, Sesarman A, Oswald E, Feldrihan V, Fritsch A, Hashimoto T, et al. Cross-reactivity of autoantibodies from patients with epidermolysis bullosa acquisita with murine collagen VII. *Cell Mol Life Sci* 2010;67:1343-51.
- Egami S, Yamagami J, Amagai M. Autoimmune bullous skin diseases, pemphigus and pemphigoid. *J Allergy Clin Immunol* 2020;145:1031-47.
- Faccio R, Creмасco V. PLCy2: where bone and immune cells find their common ground. *Ann N Y Acad Sci* 2010;1192:124-30.
- Futosi K, Németh T, Pick R, Vántus T, Walzog B, Mócsai A. Dasatinib inhibits proinflammatory functions of mature human neutrophils. *Blood* 2012;119:4981-91.
- Futosi K, Kása O, Szilveszter KP, Mócsai A. Neutrophil phospholipase Cy2 drives autoantibody-induced arthritis through the generation of the inflammatory microenvironment. *Arthritis Rheumatol* 2021;73:1614-25.
- Gammon WR, Merritt CC, Lewis DM, Sams WM, Jr., Carlo JR, Wheeler CE, Jr. An in vitro model of immune complex-mediated basement membrane zone separation caused by pemphigoid antibodies, leukocytes, and complement. *J Invest Dermatol* 1982;78:285-90.
- Graham DB, Robertson CM, Bautista J, Mascarenhas F, Diacovo MJ, Montgrain V, et al. Neutrophil-mediated oxidative burst and host defense are controlled by a Vav-PLCy2 signaling axis in mice. *J Clin Invest* 2007;117:3445-52.
- Gross S, Gammon ST, Moss BL, Rauch D, Harding J, Heinecke JW, et al. Bioluminescence imaging of myeloperoxidase activity in vivo. *Nat Med* 2009;15:455-61.
- Hashimoto A, Takeda K, Inaba M, Sekimata M, Kaisho T, Ikehara S, et al. Cutting edge: essential role of phospholipase Cy2 in B cell development and function. *J Immunol* 2000;165:1738-42.
- Hundt JE, Iwata H, Pieper M, Pfundl R, Bieber K, Zillikens D, et al. Visualization of autoantibodies and neutrophils in vivo identifies novel checkpoints in autoantibody-induced tissue injury. *Sci Rep* 2020;10:4509.
- Ichise H, Ichise T, Yoshida N. Phospholipase Cy2 is required for luminal expansion of the epididymal duct during postnatal development in mice. *PLoS One* 2016;11:e0150521.

- Jackson JT, Mulazzani E, Nutt SL, Masters SL. The role of PLC $\gamma$ 2 in immunological disorders, cancer and neurodegeneration. *J Biol Chem* 2021;100905.
- Jakus Z, Simon E, Frommhold D, Sperandio M, Mócsai A. Critical role of phospholipase  $\text{C}\gamma$ 2 in integrin and Fc receptor-mediated neutrophil functions and the effector phase of autoimmune arthritis. *J Exp Med* 2009;206:577-93.
- Jakus Z, Simon E, Balázs B, Mócsai A. Genetic deficiency of Syk protects mice from autoantibody-induced arthritis. *Arthritis Rheum* 2010;62:1899-910.
- Kasperkiewicz M, Schmidt E. Current treatment of autoimmune blistering diseases. *Curr Drug Discov Technol* 2009;6:270-80.
- Kertész Z, Győri D, Körmendi S, Fekete T, Kis-Tóth K, Jakus Z, et al. Phospholipase  $\text{C}\gamma$ 2 is required for basal but not oestrogen deficiency-induced bone resorption. *Eur J Clin Invest* 2012;42:49-60.
- Kovács M, Németh T, Jakus Z, Sitaru C, Simon E, Futosi K, et al. The Src-family kinases Hck, Fgr, and Lyn are critical for the generation of the in vivo inflammatory environment without a direct role in leukocyte recruitment. *J Exp Med* 2014;211:1993-2011.
- Kridin K, Kneiber D, Kowalski EH, Valdebran M, Amber KT. Epidermolysis bullosa acquisita: A comprehensive review. *Autoimmun Rev* 2019;18:786-95.
- Maglie R, Hertl M. Pharmacological advances in pemphigoid. *Curr Opin Pharmacol* 2019;46:34-43.
- Mao D, Epple H, Uthgenannt B, Novack DV, Faccio R. PLC $\gamma$ 2 regulates osteoclastogenesis via its interaction with ITAM proteins and GAB2. *J Clin Invest* 2006;116:2869-79.
- Martin-Nalda A, Fortuny C, Rey L, Bunney TD, Alsina L, Esteve-Sole A, et al. Severe Autoinflammatory Manifestations and Antibody Deficiency Due to Novel Hypermorphic PLCG2 Mutations. *J Clin Immunol* 2020;40:987-1000.
- Mócsai A, Zhou M, Meng F, Tybulewicz VL, Lowell CA. Syk is required for integrin signaling in neutrophils. *Immunity* 2002;16:547-58.
- Mócsai A, Zhang H, Jakus Z, Kitaura J, Kawakami T, Lowell CA. G-protein-coupled receptor signaling in Syk-deficient neutrophils and mast cells. *Blood* 2003;101:4155-63.
- Mócsai A. Diverse novel functions of neutrophils in immunity, inflammation, and beyond. *J Exp Med* 2013;210:1283-99.
- Moran-Villasenor E, Saez-de-Ocariz M, Torrelo A, Arostegui JI, Yamazaki-Nakashimada MA, Alcantara-Ortigoza MA, et al. Expanding the clinical features of autoinflammation and phospholipase  $\text{C}\gamma$ 2-associated antibody deficiency and immune dysregulation by description of a novel patient. *J Eur Acad Dermatol Venereol* 2019;33:2334-9.
- Németh T, Futosi K, Hably C, Brouns MR, Jakob SM, Kovács M, et al. Neutrophil functions and autoimmune arthritis in the absence of p190RhoGAP: Generation and analysis of a novel null mutation in mice. *J Immunol* 2010;185:3064-75.
- Németh T, Futosi K, Sitaru C, Ruland J, Mócsai A. Neutrophil-specific deletion of the CARD9 gene expression regulator suppresses autoantibody-induced inflammation in vivo. *Nat Commun* 2016;7:11004.
- Németh T, Mócsai A. Feedback amplification of neutrophil function. *Trends Immunol* 2016;37:412-24.
- Németh T, Vartic O, Sitaru C, Mócsai A. The Syk tyrosine kinase is required for skin inflammation in an in vivo mouse model of epidermolysis bullosa acquisita. *J Invest Dermatol* 2017;137:2131-9.
- Neves JF, Doffinger R, Barcena-Morales G, Martins C, Papapietro O, Plagnol V, et al. Novel PLCG2 Mutation in a Patient With APLAID and Cutis Laxa. *Front Immunol* 2018;9:2863.
- Nonne C, Lenain N, Hechler B, Mangin P, Cazenave JP, Gachet C, et al. Importance of platelet phospholipase  $\text{C}\gamma$ 2 signaling in arterial thrombosis as a function of lesion severity. *Arterioscler Thromb Vasc Biol* 2005;25:1293-8.
- Novice T, Kariminia A, Del Bel KL, Lu H, Sharma M, Lim CJ, et al. A Germline Mutation in the C2 Domain of PLC $\gamma$ 2 Associated with Gain-of-Function Expands the Phenotype for PLCG2-Related Diseases. *J Clin Immunol* 2020;40:267-76.

- Ombrello MJ, Remmers EF, Sun G, Freeman AF, Datta S, Torabi-Parizi P, et al. Cold urticaria, immunodeficiency, and autoimmunity related to PLCG2 deletions. *N Engl J Med* 2012;366:330-8.
- Schmidt E, Zillikens D. Pemphigoid diseases. *Lancet* 2013;381:320-32.
- Sezin T, Krajewski M, Wutkowski A, Mousavi S, Chakievska L, Bieber K, et al. The Leukotriene B4 and its Receptor BLT1 Act as Critical Drivers of Neutrophil Recruitment in Murine Bullous Pemphigoid-Like Epidermolysis Bullosa Acquisita. *J Invest Dermatol* 2017;137:1104-13.
- Sitaru C, Mihai S, Otto C, Chiriac MT, Hausser I, Dotterweich B, et al. Induction of dermal-epidermal separation in mice by passive transfer of antibodies specific to type VII collagen. *J Clin Invest* 2005;115:870-8.
- Szilveszter KP, Németh T, Mócsai A. Tyrosine kinases in autoimmune and inflammatory skin diseases. *Front Immunol* 2019;10:1862.
- Tassi I, Presti R, Kim S, Yokoyama WM, Gilfillan S, Colonna M. Phospholipase C $\gamma$ 2 is a critical signaling mediator for murine NK cell activating receptors. *J Immunol* 2005;175:749-54.
- Turcan I, Jonkman MF. Blistering disease: insight from the hemidesmosome and other components of the dermal-epidermal junction. *Cell Tissue Res* 2015;360:545-69.
- Wang D, Feng J, Wen R, Marine JC, Sangster MY, Parganas E, et al. Phospholipase C $\gamma$ 2 is essential in the functions of B cell and several Fc receptors. *Immunity* 2000;13:25-35.
- Wen R, Jou ST, Chen Y, Hoffmeyer A, Wang D. Phospholipase C $\gamma$ 2 is essential for specific functions of Fc $\epsilon$ R and Fc $\gamma$ R. *J Immunol* 2002;169:6743-52.
- Wonerow P, Pearce AC, Vaux DJ, Watson SP. A critical role for phospholipase C $\gamma$ 2 in  $\alpha$ <sub>IIb</sub> $\beta$ <sub>3</sub>-mediated platelet spreading. *J Biol Chem* 2003;278:37520-9.
- Yu P, Constien R, Dear N, Katan M, Hanke P, Bunney TD, et al. Autoimmunity and inflammation due to a gain-of-function mutation in phospholipase C $\gamma$ 2 that specifically increases external Ca<sup>2+</sup> entry. *Immunity* 2005;22:451-65.
- Zhou Q, Lee GS, Brady J, Datta S, Katan M, Sheikh A, et al. A hypermorphic missense mutation in PLCG2, encoding phospholipase C $\gamma$ 2, causes a dominantly inherited autoinflammatory disease with immunodeficiency. *Am J Hum Genet* 2012;91:713-20.

Graphical abstract

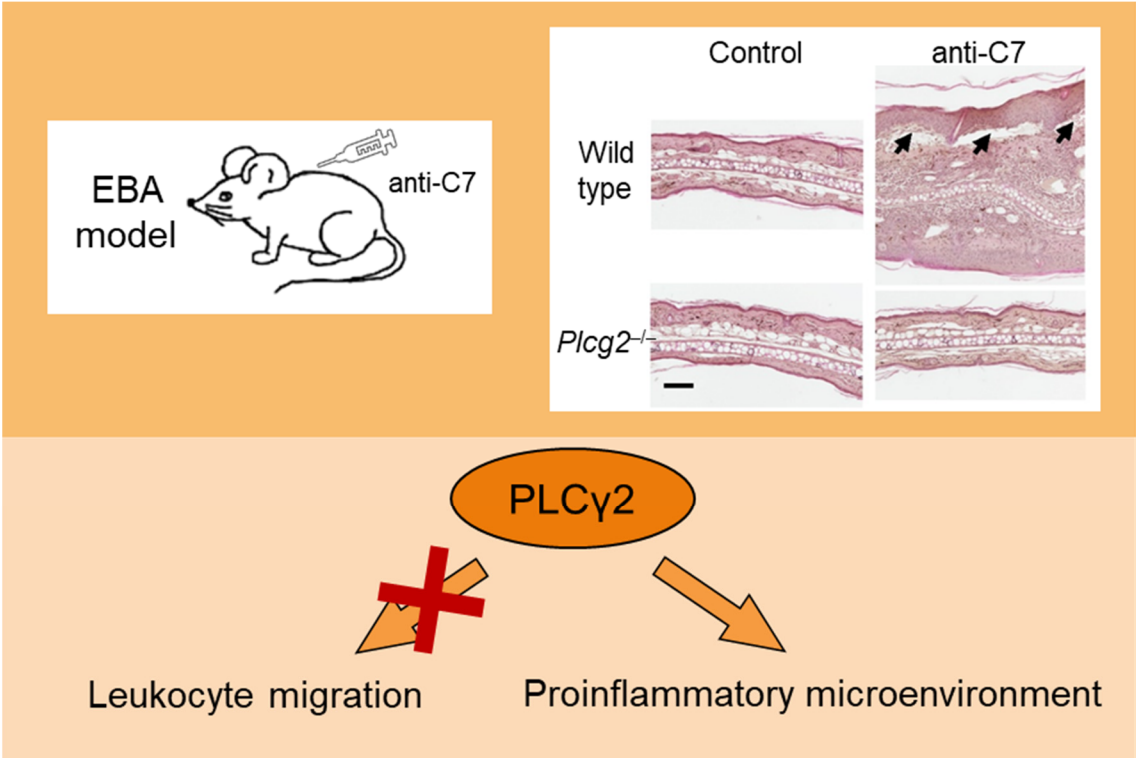


**Figure 1**

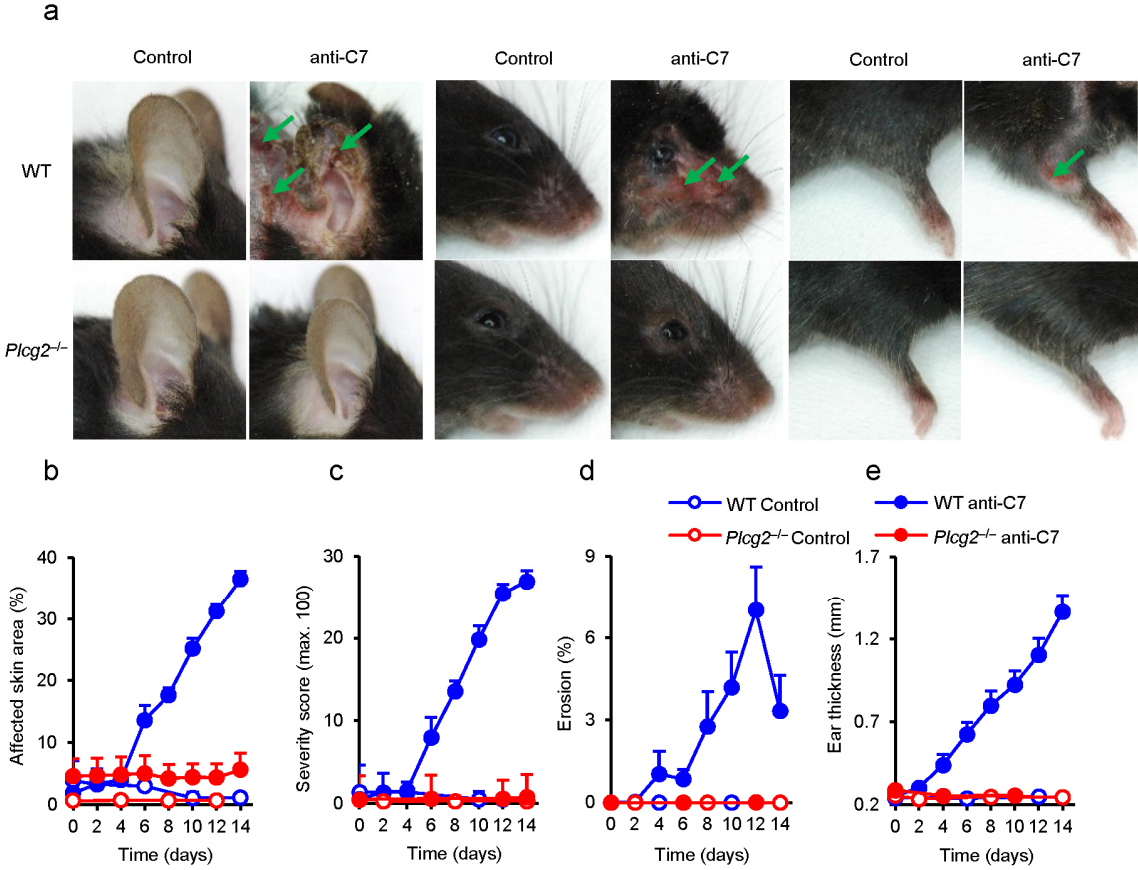


**Figure 2**

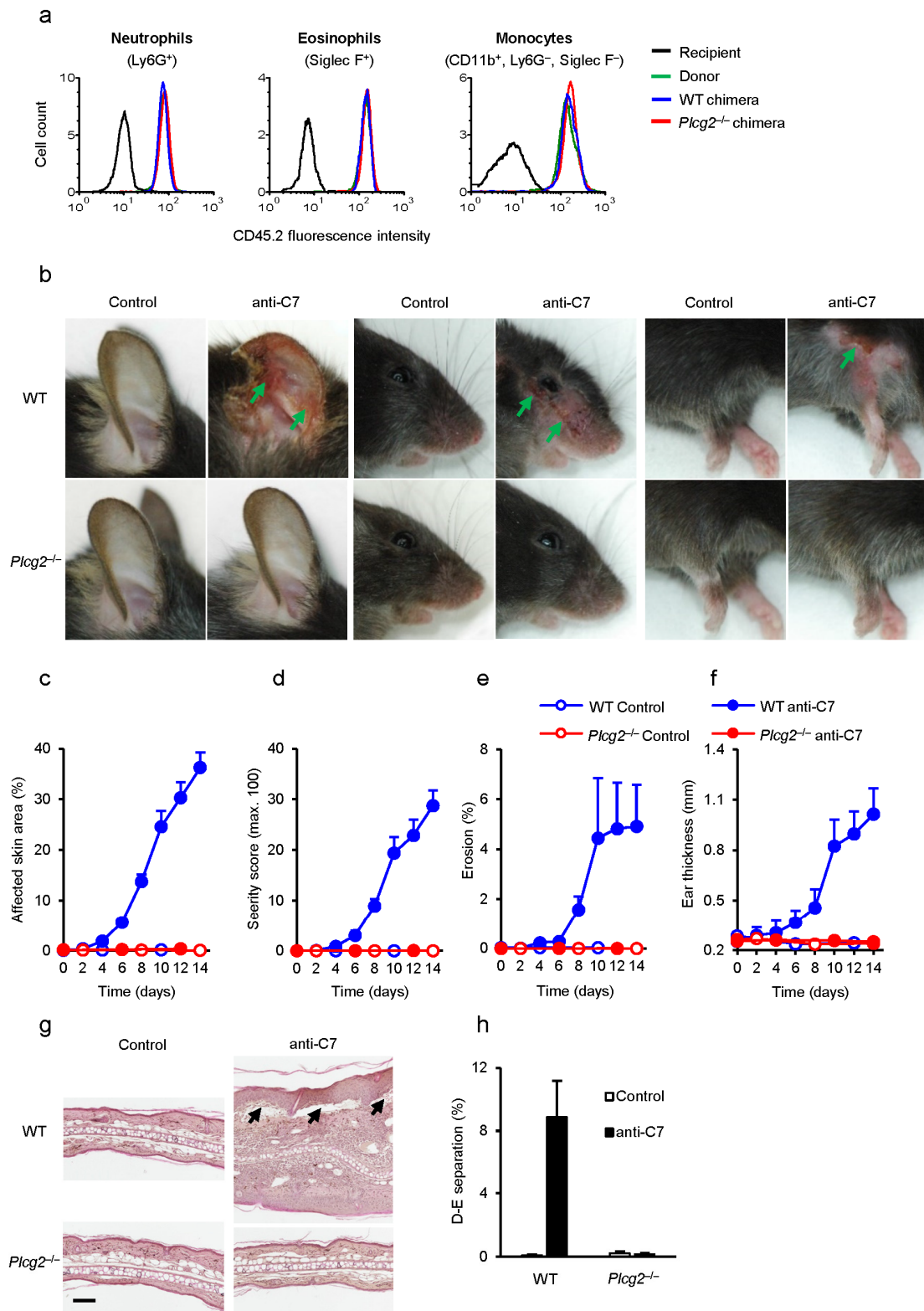


**Figure 3**

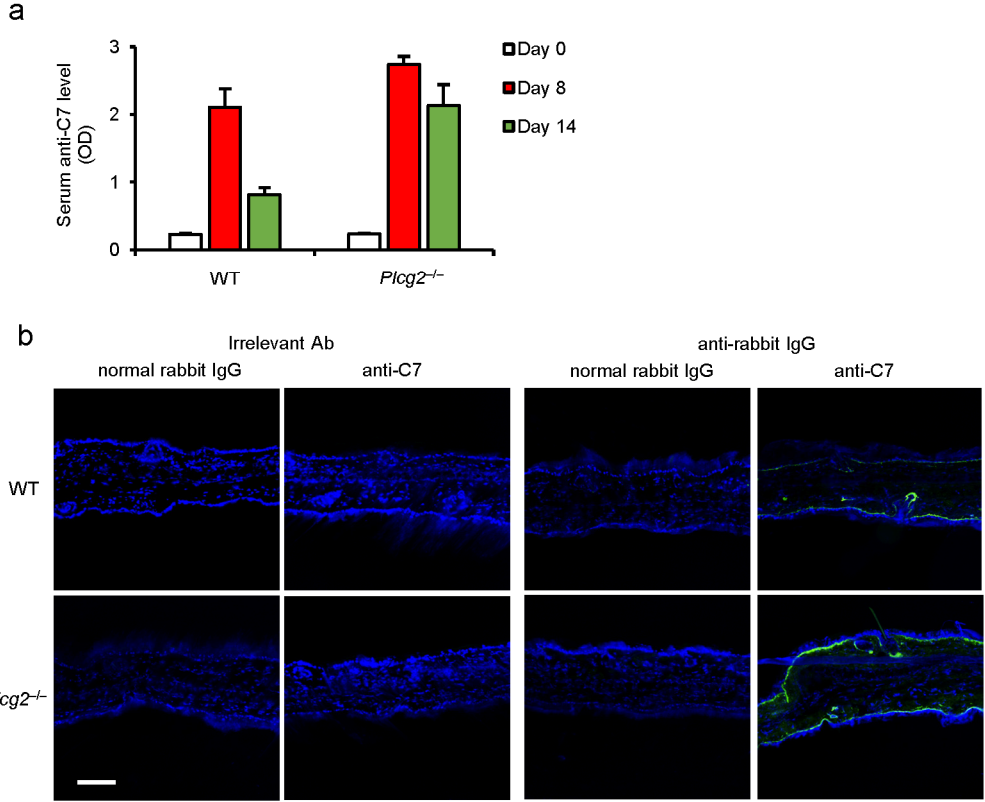




**Figure 5**

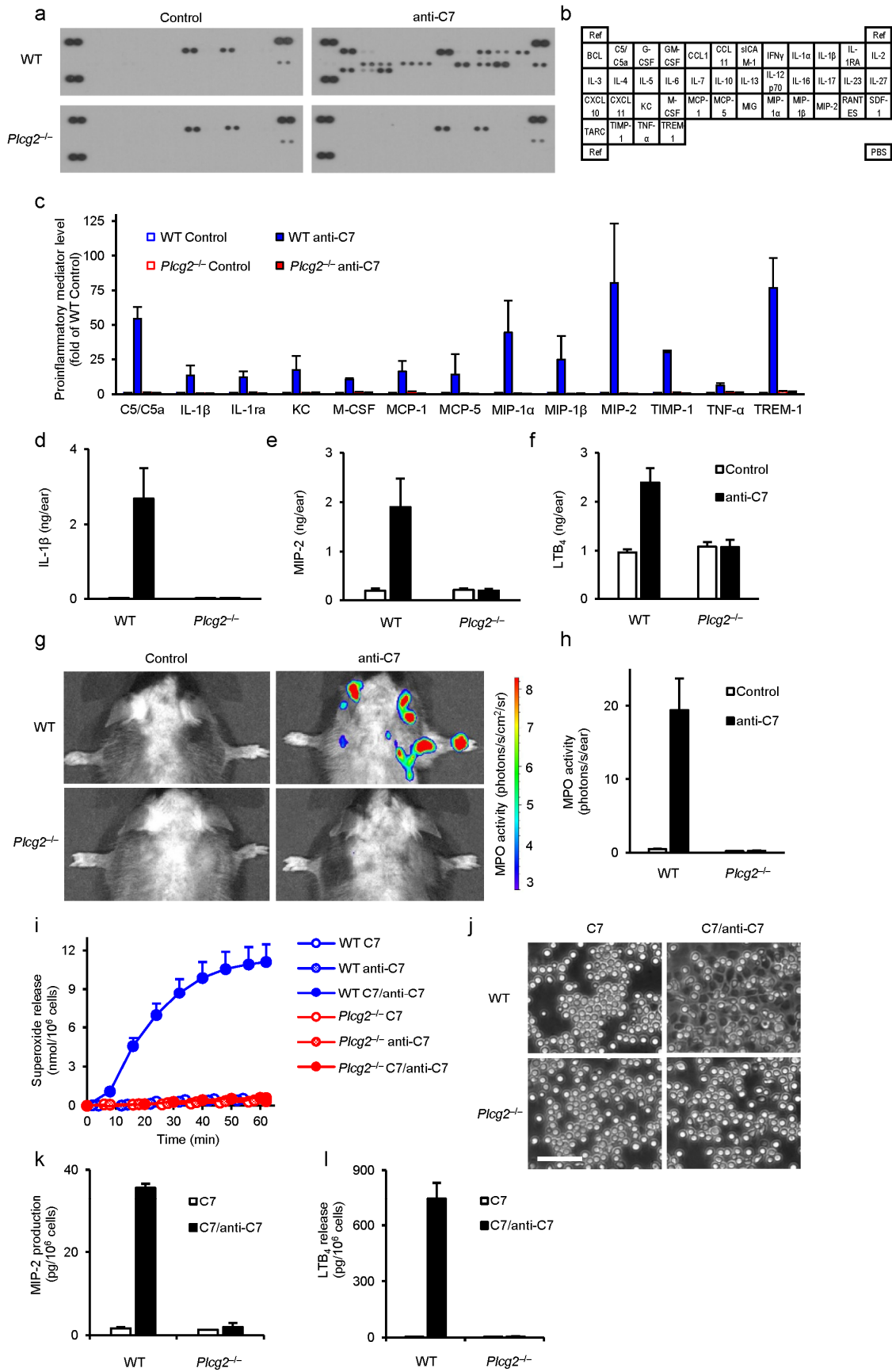


**Figure 6**

